

# AN EXPERIMENTAL INVESTIGATION OF SOLID GRAINS FLOW OVER CYLINDRICAL SURFACES

BY

MOHAMMED A. HABIB and SHEDID H. SHAMS EL-DIN.  
MECHANICAL POWER ENG. FACULTY OF ENG.  
MENOUIYA UNIVERSITY, SHIBEN EL-KOM, EGYPT.

## ABSTRACT:

An experimental investigation of solid grains flow over cylindrical surfaces has been carried out to study the flow characteristics at different operating conditions. The present study assists in understanding the grains flow mechanism and flow separation phenomenon occurring at the rear part of the cylinder. Experimental data are obtained with rice grains used as the solid working material. Effects of both grains mean velocity and diameter ratio on the geometric dimensions of front stagnant region, rear air region and effective working surface are investigated. Visual studies of the flow patterns are also discussed. Velocity distribution around the cylinder is obtained for different diameter ratios from typical flow patterns produced by black tracer technique. The mean particles velocity ranged from 2 to 18 mm/sec and the diameter ratio from 0.05 to 0.30. The results have shown that the flow characteristics depend strongly on the grain layers mean velocity and the diameter ratio.

## 1. INTRODUCTION:

In recent years there has been an increase in the use of efficient heat recovery systems; heat pipe-heat exchanger HPHE, in the field of heat treatment processes, for example, drying or cooling agricultural products [1-5] and different industrial processes [6, 7]. Savings have been found possible by reclaiming heat from industrial exhausts, e.g., exhausts from boilers, furnaces and industrial kilns [8]. For drying purposes, the circular cylinder in cross flow is the most extensively used element in the structure of HPHE. It is important to study the grains flow pattern characteristics of the agricultural products over these surfaces which make it possible to predict the main features of the heat transfer rates along the cylindrical surfaces of the heat pipe elements. However, visualization study of the flow pattern will aid in

---

MANUSCRIPT RECEIVED FROM DR. M.A. HABIB AT: 16/5/1995,  
ACCEPTED AT: 30/10/1995, PP 35 - 55  
ENGINEERING RESEARCH BULLETIN, VOL. 19, NO. 1, 1996  
MENOUIYA UNIVERSITY, FACULTY OF ENGINEERING,  
SHEBIEN EL-KOM, EGYPT. ISSN 1110-1180

determining the relevant transversal and longitudinal motions and hence, the maximum of heat transfer rates.

Most of the published literature on the flow patterns over cylindrical surfaces are applicable to fluid flow. There have been very few investigations devoted to a single cylinder or tube banks, HPHE, placed transversely in the direction of the solid grains flow [4, 5]. For a single cylinder, a clear explanation of the flow pattern at different regions; stagnant and rear air regions and the influence of the main parameters, layers flow velocity as well as cylinder diameter has not been provided. In addition, the determination of the effective working surface under the influence of different parameters has not been investigated. The local velocity distribution of solid particles also needs to be studied. Therefore, the present study aims at investigating these factors and thus, fill in some gap in the literature.

## 2. EXPERIMENTAL APPARATUS AND PROCEDURES:

The experiments were performed in an apparatus which has a test section of a vertical squared duct 200x200 mm and 1200 mm height as shown in Fig. 1. The wall of the duct was prepared from Plexiglas to permit visual observations and consequently recording the flow process. Rice grains were used as the solid working material. The density of the grains is 1008 kg/m<sup>3</sup>. Six different cylinders were tested in the present study with diameters, D, of 10, 20, 30, 40, 50 and 60 mm, respectively. The corresponding diameter ratio D/b; cylinder diameter to duct width are 0.05, 0.10, 0.15, 0.20, 0.25 and 0.30, respectively. In order to avoid the wall effects, the test cylinder was located in the center of the test section. Experimental results were obtained for particles mean velocity  $V_m$  ranging from 2 to 18 mm/sec. Particles mean velocity were controlled with the aid of a slide gate located at the bottom part of the test section. Another slide gate was located at the upper part to maintain the required flow discharge from the hopper and facilitate the addition of the thin black layer to the main flow. Rice grains mean velocity was determined by measuring the time for grains to flow through a certain known distance. The distance was measured from the location of the black thin layer in the far upstream to the horizontal centerline of the cylinder ( $x/D=0$ ). The maximum velocity of grains was obtained at the horizontal centerline of the cylinder with the aid of the continuity equation. Since the flow is steady, the velocity increases as the flow area decreases. At this location; ( $x/D=0$ ), the flow area is the minimum. Therefore, the velocity would be maximum. The maximum velocity can be obtained as follows:

$$V_{\max} = V_m \cdot l / (l - D) \quad (1)$$

Where  $V_m$  is the grains mean velocity,  $l$  and  $(l - D)$  are the total and the free flow widths of the duct.

The continuity equation was also applied at different locations to determine the grains local velocity in the upstream and downstream of the cylinder using the measured mean velocity, the total and the free flow widths of the duct. Local velocity distribution around the cylinder was determined from the recorded flow patterns in such a way that the vertical distance  $x_1$  was abstracted from the maximum velocity in the upstream of the cylinder while it is added in the downstream direction. Figure 2 presents the vertical distances  $x_1$  in the upstream and downstream of the cylinder at different angular positions. The maximum relative error in measuring the layers mean velocity is less than 3 %. The total effective working surface  $\epsilon$  can be determined as follows:

$$\epsilon = (2 \cdot \theta_1 \cdot \Pi \cdot D) / 360 \quad (2)$$

Where  $\theta_1$  is the angular position between the stagnation and the separation points and D is the diameter of the cylinder.

The test procedures were as follows:

- 1- The typical flow field produced by the flowing solid particles over cylinders was obtained using the black tracer technique by adding a thin layer of black powder to the flowing material upstream of the test section.
- 2- When the thin black layer outer edges reach the horizontal centerline of the cylinder, the lower slide gate was closed and the flow pattern over the cylinder was photographed and recorded using a transparent paper.
- 3- At the same grain flow rate, a new black layer was added and the grains motion was resumed and step 2 was repeated.
- 4- The upper slide gate was opened and the flow particles were permitted to fill again the test section.
- 5- For each experimental run a new black layer was used and the flow pattern was photographed and recorded.

### 3. RESULTS AND DISCUSSIONS:

In practice, it is required to operate HPHE systems such that the grain particles are not over heated. Therefore, the system must be arranged in such a way that the flow rate of grains in the condenser zone be continuous and dead zones where grain particles remain stagnant should not be allowed. Under these conditions it is necessary to estimate the required flow velocity of particles. However, it was found in [4] that the best performance of drying process occurs when the velocity of flowing grain layers ranges between 2-24 mm/sec, depending upon the diameter of the cylinder used. Therefore, in the present study, the flow particles mean velocity is chosen within this range.

### 3.1. Flow Visualization:

The black tracer technique was found to be very useful to observe the grain layers flow around the surface of the cylinder. The photographic view of the flow patterns was taken for diameter ratios of 0.05 and 0.30 ( $D=10$  and  $60$  mm) at layers mean velocities of 2 and 18 mm/sec. From the typical patterns of the flow field indicated by the photographs shown in Fig. 3, three main regions are distinguished:

- 1- Dead (stagnant) region: this region is formed on the front part of the cylinder. It is characterized by a stagnant packed layers.
- 2- Separation region: this region which is relatively smaller than the stagnant region and is formed in the rear part of the cylinder. This region does not contain any solid particles in direct contact with the surface. Hence, it is often called the rear air region.
- 3- Attachment region: this region which extends along the sides of the cylinder includes solid particles in continuous motion. Figure 3 also shows the flow patterns at  $x/D=0.33$  and  $x/D=1$ , respectively. It can be seen that the black thin layer moves downstream and the particles flow along the sides of the cylinder.

Factors affecting the characteristics of different regions are the grain layers mean velocity and the diameter ratio. The effect of the mentioned factors on the characteristics of the dead and the rear air regions were obtained from the dimensions of these regions. These dimensions include the height ratio ( $L/D$ ), dead region height to cylinder diameter ratio, the depth ratio ( $Z/D$ ), rear region depth to cylinder diameter ratio, and area ratios; ( $A_d/A_c$ ) dead to cylinder areas ratio and ( $A_r/A_c$ ) rear to cylinder areas ratio. For a given cylinder diameter, increasing the layer mean velocity produces a clearly visible reduction in the dimensions of both stagnant and rear air regions. However, the effect of the diameter ratio produces an opposite effect. Moreover, the dimensions of the rear air region are smaller than that found for the stagnant region. For all flow conditions, stationary layers of particles always exist on the surface of the cylinder. At layers mean velocity greater than 6 mm/sec, there are better mixing of grains and an increase in particles motion occur especially on both sides of the cylinder. The particles at both sides are able to move faster. This makes the particles acquire higher kinetic energy and partially fill the rear air region and thus results a decrease in its depth and area. It should be born in mind that reverse grain particles flow is not observed downstream of the cylinder compared with that in the case of fluids flow around the cylinder. Further details about the effect of both the mean velocity and the diameter ratio on these regions appear in the following sections.

### 3.2. Flow Pattern Characteristics:

In order to study the flow pattern characteristics, the effect of the layers mean velocity and the diameter ratio on the dimensions of the dead, the rear air regions and the effective working surface were discussed. The layers local velocity distributions were first given.

#### 3.2.1. Layers Local Velocity Distribution:

Figures 4 a and b present the distribution of grain layers local velocity  $V_1$  and  $V_1/V_m$  against the height of the test section to cylinder diameter ratio ( $X/D$ ) at three values of grains mean velocity namely; 2, 9 and 18 mm/sec for diameter ratios ( $D/b$ ) of 0.05, 0.10, 0.20 and 0.30, respectively. From these figures, it can be seen that the distribution has a central port which is parabolic-like profile. It exhibits symmetry with respect to the horizontal axis. The figures indicate that the local mean velocity increases with increasing the diameter ratio and the rate of increase becomes higher at  $D/b = 0.30$ . The effect of mean velocity is small compared with the diameter ratio.

The local velocity distributions at mean velocities of 2 and 18 mm/sec for various diameter ratios are shown in Figs. 5 and 6, respectively. It can be seen that, for rice grains the velocity distribution curves have a parabolic form with a peak in the front part of the cylinder (at  $\theta=0^\circ$ ). The peak of the parabola is gradually reduced with increasing the diameter ratio. This clearly can be observed at  $V_m=18$  mm/sec. It can be noticed from Fig. 5 that in the range of  $\theta$  between  $70^\circ$  and  $85^\circ$ , the particle local velocity decreases with increasing the diameter ratio and in the range between  $85^\circ$  and  $153^\circ$  in the rear parts, it increases. This is due to the existence of the stagnant layers that formed on the front part of the cylinder which increases with increasing ( $D/b$ ). The grain particles tend to decelerate as they pass near this layers then accelerate as they pass around the sides and the rear portions. This results in a decrease in layers velocity on the front part and an increase on the sides and rear portions. Such a trend of velocity distribution is obtained also for layers mean velocity of 18 mm/sec, Fig. 6. From this figure it can be noticed that the increase in the local velocity with decreasing the diameter ratio in the front part occurs between  $0^\circ$  and  $75^\circ$  where the kinetic energy of the layers becomes higher, compared with the case of  $V_m=2$  mm/sec. This implies that the cross sectional area of the stagnant layers is decreased and the angular position is shifted upstream from  $85^\circ$  to  $75^\circ$  with increasing the mean velocity from 2 to 18 mm/sec. A gradual shift of the separation point in the upstream direction occurs at angles between  $113^\circ$  and  $138^\circ$ .

### 3.2.2. Dead region characteristics:

Figures 7 and 8 illustrate the effect of diameter ratio ( $D/b$ ) on the dead region geometric parameters;  $(L/D)$  and  $(A_d/A_c)$ , respectively. It can be seen that both  $(L/D)-V_m$  and  $(A_d/A_c)-V_m$  relations have similar trends. However, at  $D/b=0.05$ , both  $(L/D)$  and  $(A_d/A_c)$  have considerably higher values compared to that for other diameter ratios. This means that the density of grain layers that accumulated on the front part with respect to its cylinder diameter is higher than that for other diameters. The increase of grain layers mean velocity leads to a decrease in both of  $(L/D)$  and  $(A_d/A_c)$  and these ratios are decreased with increasing diameter ratio as shown in Figs. 9 and 10.

The behavior described above is attributed to the fact that the increase in grain velocity reduces the stagnant layers by continuous erosion and hence the geometric parameters of the accumulated layers  $(L/D)$  and  $(A_d/A_c)$  are sharply decreased. The results indicate that, at low diameter ratio,  $D/b = 0.05$ ,  $(L/D)$  decreases from 0.80 to 0.70 when layers mean velocity is increased from 2 to 18 mm/sec, while these ratios are reduced from 0.57 to 0.44 when diameter ratio increases to 0.30. Also, the parameter  $(A_d/A_c)$  is decreased from 0.47 to 0.30 at  $D/b=0.05$ , while it is decreased from 0.26 to 0.15 at  $D/b=0.30$  when the grain mean velocity is increased from 2 to 18 mm/sec.

On the other hand, the density of stagnant layers that accumulated on the front part is proportional to the diameter of the cylinder but the rate of increase for both  $L$  and  $A_d$  are not equal to the corresponding increase in  $D$  and  $A_c$ . However, both  $(L/D)$  and  $(A_d/A_c)$  ratios are increased with decreasing cylinder diameter and the rate of increasing is higher at smaller diameters. In addition, the results show that the dead region covers between 14.3 % and 34.6 % of the cylinder surface, depending on the layers mean velocity and the tested diameter.

### 3.2.3. Separation region characteristics:

The separated flow region characteristics, at the rear part of the cylinder, are given in Figs. 11 and 12. These figures present the effect of diameter ratio ( $D/b$ ) on the geometric parameters  $(Z/D)$  and  $(A_r/A_c)$ . It is clear that  $(Z/D)$  and  $(A_r/A_c)$  vary with layers mean velocity in a non-linear fashion, when compared with that for the front part of the cylinder. Moreover, the trend is not the same for different cylinder diameters. For diameter ratios in the range of  $0.20 < D/b < 0.30$ , both  $(Z/D)$  and  $(A_r/A_c)$  increase to a maximum value up to a

certain velocity ( $V_m = 6$  mm/sec) and then they decrease with further increase in layers mean velocity. For  $0.05 < D/b < 0.15$ , both  $(Z/D)$  and  $(A_r/A_c)$  decrease gradually with increasing velocity. At constant mean velocity, these ratios decrease with increasing the diameter ratio as shown in Figs. 13 and 14. Again, the smaller diameter ratio,  $D/b=0.05$ , exhibits the highest  $(Z/D)$  and  $(A_r/A_c)$  rates compared to that found for other diameter ratios. The increase in  $(Z/D)$  and  $(A_r/A_c)$  at low velocities,  $V_m < 6$  mm/sec, may be due to the decrease in the layers densities in the downstream region as the layers mean velocity increases. With further increase in layers velocity,  $V_m$  greater than 6 mm/sec, grain layers kinetic energy effects are dominant and the particles in the downstream sides of the cylinder are able to move faster and partially fill the rear air region. This results in a decrease in its depth and area. It has been found that the separation region represents between 13 % and 32.8 % of the cylinder surface, depending on the flow velocity and diameter ratio.

#### 3.2.4. Effective working surface characteristics:

Figures 15 and 16 show the effect of diameter ratio ( $D/b$ ) and grains mean velocity  $V_m$  on the effective working surface  $\epsilon$ . It can be noticed that  $\epsilon$  varies linearly with grains mean velocity  $V_m$ . One can distinguish two regions;  $0.05 < D/b < 0.10$  and  $0.15 < D/b < 0.30$  where the increase in  $\epsilon$  is more remarkable. However, increasing the grains mean velocity  $V_m$  leads to an increase in  $\epsilon$ . Furthermore, at constant value of  $V_m$  the effective working surface increases with increasing the diameter ratio, but the rate is higher for  $0.10 < D/b < 0.15$ . For diameter ratio of  $0.05 < D/b < 0.10$ , the rate of increase in  $\epsilon$  ranges from 5.7 % to 7.1 % while this rate changes from 8.6 % to 10 % when  $0.15 < D/b < 0.30$ .

As discussed earlier, increasing  $V_m$  leads to a reduction in the geometric dimensions of the dead and rear air regions and to an increase in the effective working surface. On the other hand, increasing  $D$ , leads to an increase in the attachment surface where the angular spacing,  $2\theta_1$ , between the front stagnation points and the points of separation increases. The results in Fig. 16 indicate that in the range of  $0.05 < D/b < 0.10$ , the layers of the grains flow around the sides of the cylinder at angles ranged from  $164^\circ$  to  $180^\circ$ , which fully covers 45.5 to 50 % of the cylinder surface, while these angles ranged from  $188^\circ$  to  $214^\circ$  corresponding to 52.4 to 59.8 % of the cylinder surface in the range of  $0.15 < D/b < 0.30$ . The attachment surface increases suddenly by about 12 % to 13.3 % when the cylinder diameter increases from 20 to 30 mm, while in the other range of diameters the rate of increase does not exceed 4 %.

The results presented in this study suggest that the minimum heat transfer rates will occur at the front stagnation points around the angular positions between  $\theta = 52^\circ$  and  $125^\circ$ . Furthermore, the maximum values of heat transfer rates would occur at the region of attachment in the flow field between  $\theta = 110^\circ$  and  $153^\circ$ , where the surface of the cylinder is more exposed to the particles mixing. The behavior of such flow may be the most important factor that influences the heat transfer rates [4]. In the range between  $\theta = 85^\circ$  and  $107^\circ$  it is expected that moderate heat transfer rates occur. At the rear part of the cylinder where flow separation occurs, there is no participation in the process of heat transfer between heat pipe surface and grain layers. More investigations are needed to study how to reduce both the stagnant and separation regions in order to enhance the heat transfer rates.

This study is conducted as one of the primary and basic tests for the application of HPHE systems in the field of agricultural products heat treatment. Further experiments and additional analytical work are required to describe in more details the mechanism of solid grain materials flow over cylindrical surfaces, the flow patterns for banks of tubes in in-line and staggered arrangements and the separation phenomenon. The influence of the main flow parameters on the particles density are also of interest.

#### 4. CONCLUSIONS:

Based on the experimental results obtained during this study, the following conclusions can be stated:

1. Rice grains flow characteristics over cylindrical surfaces depend strongly on layers mean velocity and diameter ratio.
2. The velocity distribution is symmetrical about horizontal axis and has a central part which can be parabolic-like profile with a peak in the front part of the cylinder (at  $\theta=0$  deg.). In the range of  $\theta$  between  $0^\circ$  and  $85^\circ$ , the local velocity decreases with increasing the diameter ratio while it increases in the range between  $75^\circ$  and  $153^\circ$ , depending on the particles mean velocity.
3. The geometric parameters of the dead region, the height and area ratios, decrease with increasing both of the layers mean velocity and the diameter ratio. The dead region fully covers from 14.3 % to 34.6 % of the cylinder diameter, depending on the mean velocity and the tested diameter.
4. In the range of diameter ratio between 0.20 and 0.30, the geometric parameters of the rear air region, the depth and area ratios, increase with increasing the layers mean velocity up to a certain velocity ;  $V_m = 6$  mm/sec. After that they decrease with increasing mean velocity. The geometric parameters gradually decrease with increasing mean velocity in the range of diameter ratio between 0.05 and 0.15. The



separation region geometric parameters, the depth and area ratios, decrease with increasing the diameter ratio. The separation region fully covers about 13 % to 32.8 % of the cylinder surface area.

5. Effective working surface increases with increasing both the layers mean velocity and the diameter ratio. Effective working surface represents between 45.5 % to 59.8 % of the cylinder surface in the considered ranges of mean velocity and diameter ratio.

#### NOMENCLATURE:

$A_d$	Dead region area, $\text{mm}^2$ .
$A_c$	Cylinder area, $\text{mm}^2$ .
$A_r$	Rear air region area, $\text{mm}^2$ .
$b$	Duct width, mm.
$A_d/A_c$	Dead region to cylinder area ratio.
$A_r/A_c$	Rear air region to cylinder area ratio.
$D$	Cylinder diameter, mm.
$D/b$	Cylinder diameter to duct width ratio.
$L$	Dead region height, mm.
$l$	Duct width, mm.
$L/D$	Dead region height to diameter ratio.
$V_l$	Layers local velocity, mm/sec.
$V_m$	Layers mean velocity, mm/sec.
$V_{\text{max}}$	Layers maximum velocity, mm/sec.
$x_i$	Vertical distance measured from the flow pattern distribution to the centerline of the cylinder, mm.
$X$	Height of the test section measured from the centerline of the cylinder, mm.
$Z$	Rear air region depth, mm.
$Z/D$	Rear air region depth to diameter ratio.
$\epsilon$	effective working surface, percent,
$\theta$	Angular position measured from the front part of the cylinder, degree.
$\theta_i$	Angular position between the stagnation and the separation points, degree.

#### REFERENCES:

1. Dunn, P. D. and Reay, D. A.; Heat Pipes, 3 rd. ed. Oxford and New York, Pergamon Press, PP. 260-261, 1982.
2. Elson, C. R.; The Heat Pipe and Its Possible Applications in the Food Industry, Sci. and Tech. Surveys, British Food Manuf. Indus., Leatherhead, Surrey, P. 89, 1989.
3. Paikert, P.; The Heat Pipe in Heat Recovery, Air Conditioning and Drying, Rev. Prat. Froid Condit. Air, V. 30, PP. 35-40, 1977.

4. Bordo, O. G., KrethKee, B. E. and Habib, M. A.; Heat Transfer in Heat Pipes for Preheating Grains Before Drying, Tecece Dokl. Ececoyou Nauch Conf., Moscow, 26-28 May, PP. 29-31, 1987.
5. Habib, M. A.; The Use of Heat Pipes for Grains Wheat Heat Treatment, Ph. D. Thesis, Odessky Tech. Inst. Peche. Prom. Odessa, Sep. 1988.
6. Chi, S.; Heat Pipe Theory and Practice, Hemisphere Publishing Co., 1st. ed., PP. 223-234, 1976.
7. Reay, D. A.; The Use of Heat Pipes in Pressure Diecasting, IV Int. Heat Pipe Conf., Palo Alto, California, PP.434-439, 1981.
8. Reiter, S.; Industrial and Commercial Heat Recovery Systems, Van, Nostrand Reinhold Comp., New York, P. 245, 1983.
9. Balanin, B. A.; Acceleration of Solid Particles in a Channel., Eng. Phis. J., Vol. 8, No. 1, PP. 16-20, 1990.
10. Zukauskas, A. and Karni, J.; High-Performance Single Phase Heat Exchangers, 2nd. ed., New York, Hemisphere Publishing Co., PP. 187-192, 1988.
11. Eckert, E. R. and Drake, R. M.; Analysis of Heat and Mass Transfer, McGraw-Hill, New York, 1st. ed., PP. 397-403, 1972.

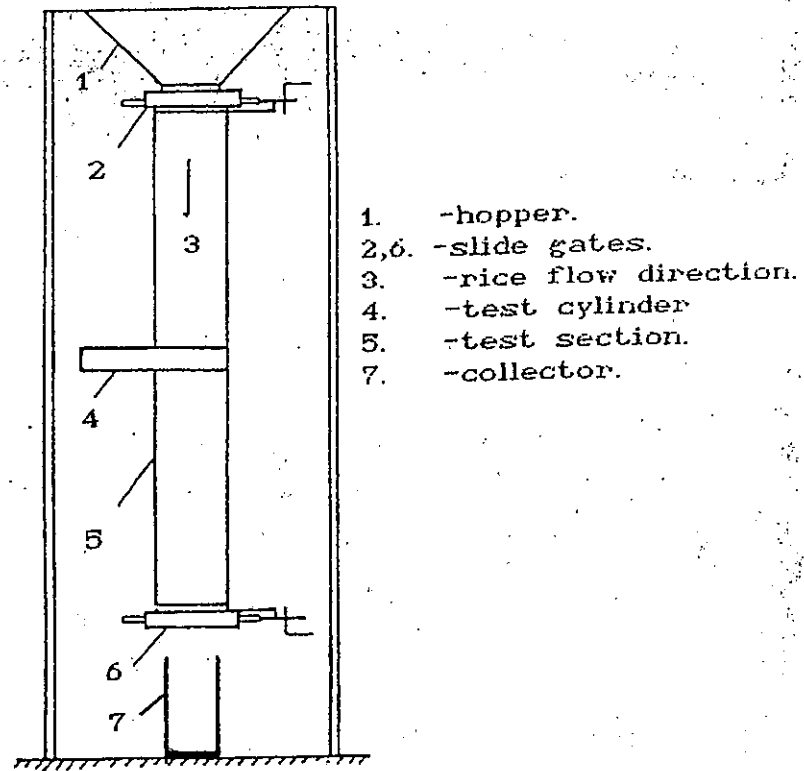


Fig.1 Schematic diagram of experimental apparatus.

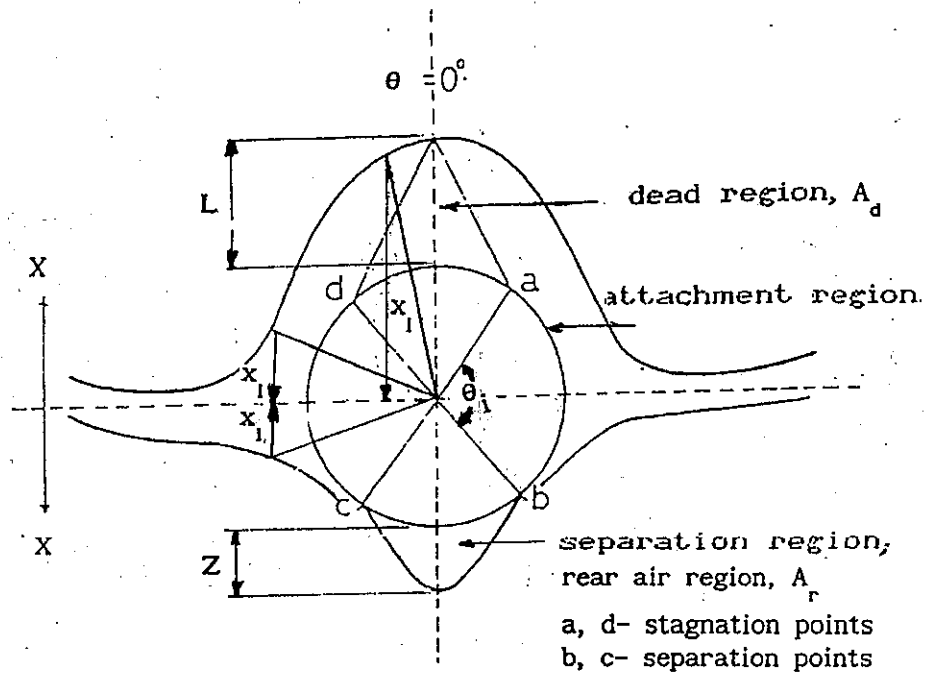
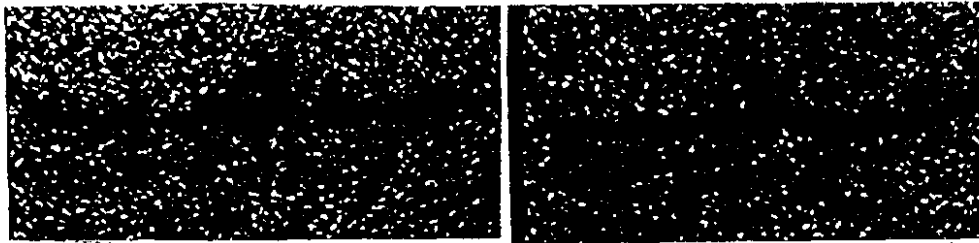


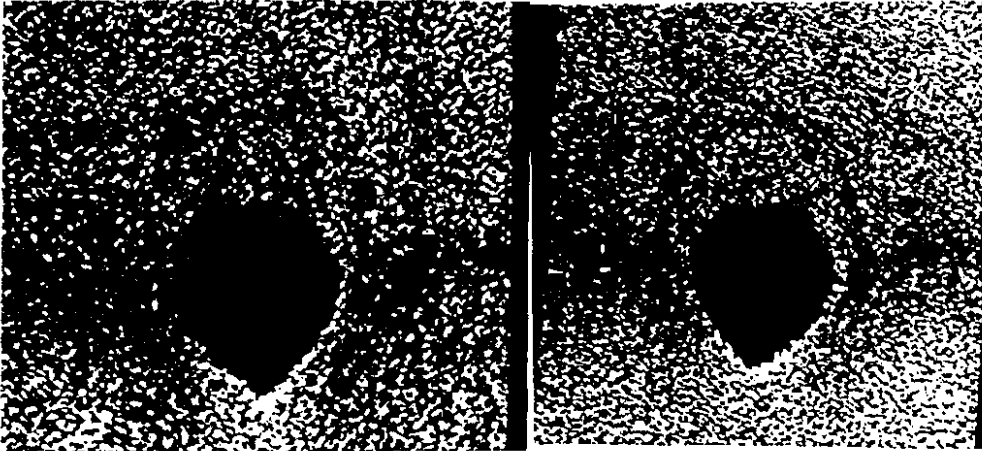
Fig.2 : Flow pattern distribution of grain layers over cylindrical surfaces.



$V_m = 2 \text{ mm/sec}$

$V_m = 18 \text{ mm/sec}$

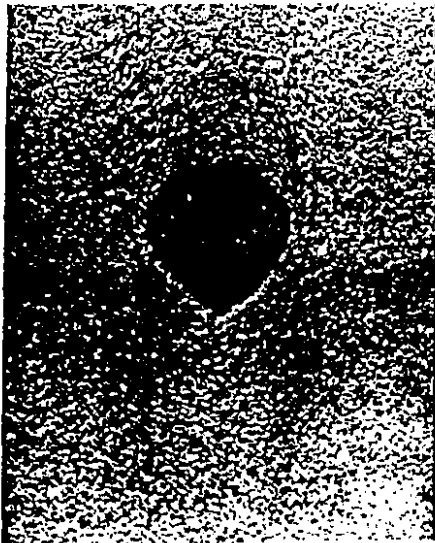
$D = 10 \text{ mm}, D/b = 0.05$



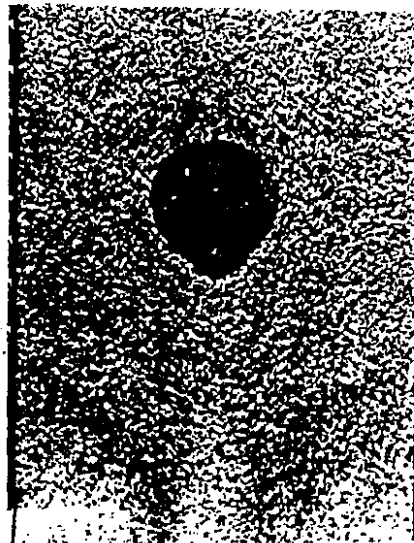
$V_m = 2 \text{ mm/sec}$

$V_m = 18 \text{ mm/sec}$

$D = 60 \text{ mm}, D/b = 0.30$



$x = 0.33 D$



$x = D$

$D = 60 \text{ mm}.$

Fig. 3: Photographs of flow patterns of rice grains over cylindrical surfaces for two different mean velocities of 2 and 18 mm/sec.

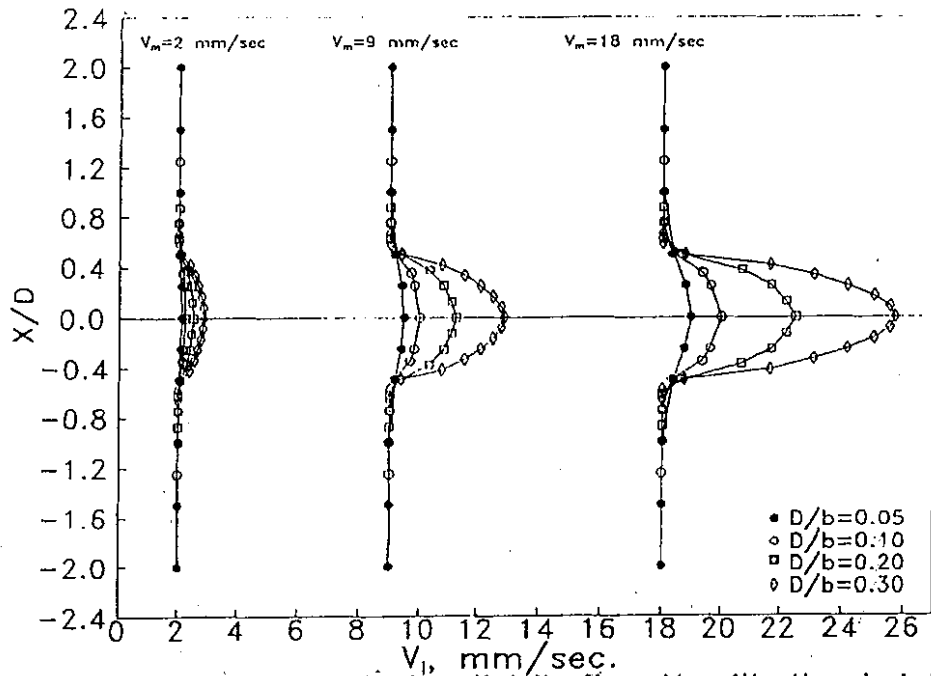


Fig.4a: Layers local velocity distribution  $V_i$  with the height of test section to cylinder diameter ratio  $X/D$ .

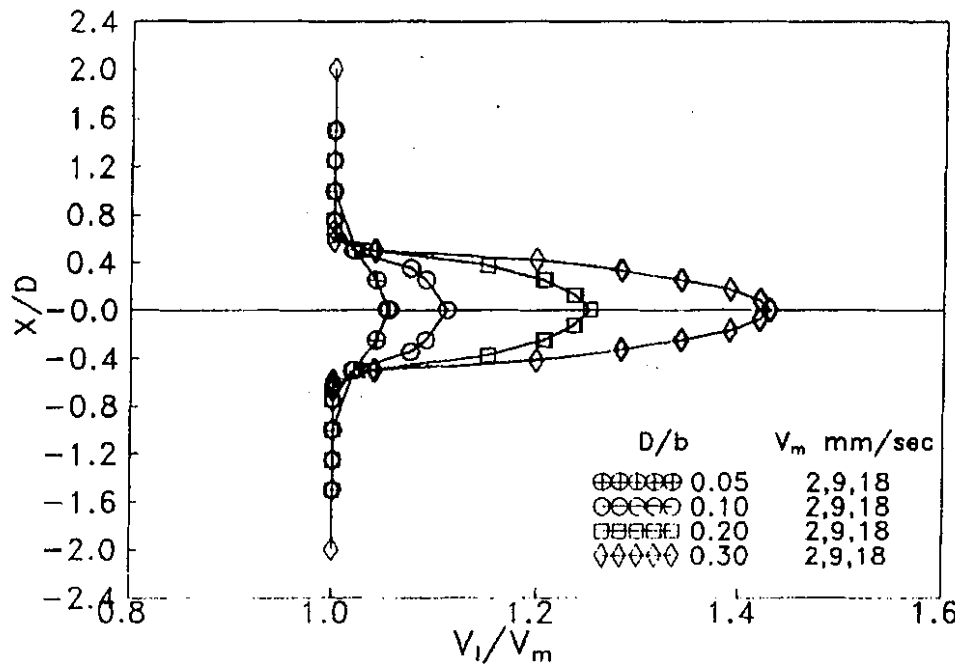


Fig.4b: Layers local velocity distribution  $V_i/V_m$  with the height of test section to cylinder diameter ratio  $X/D$ .

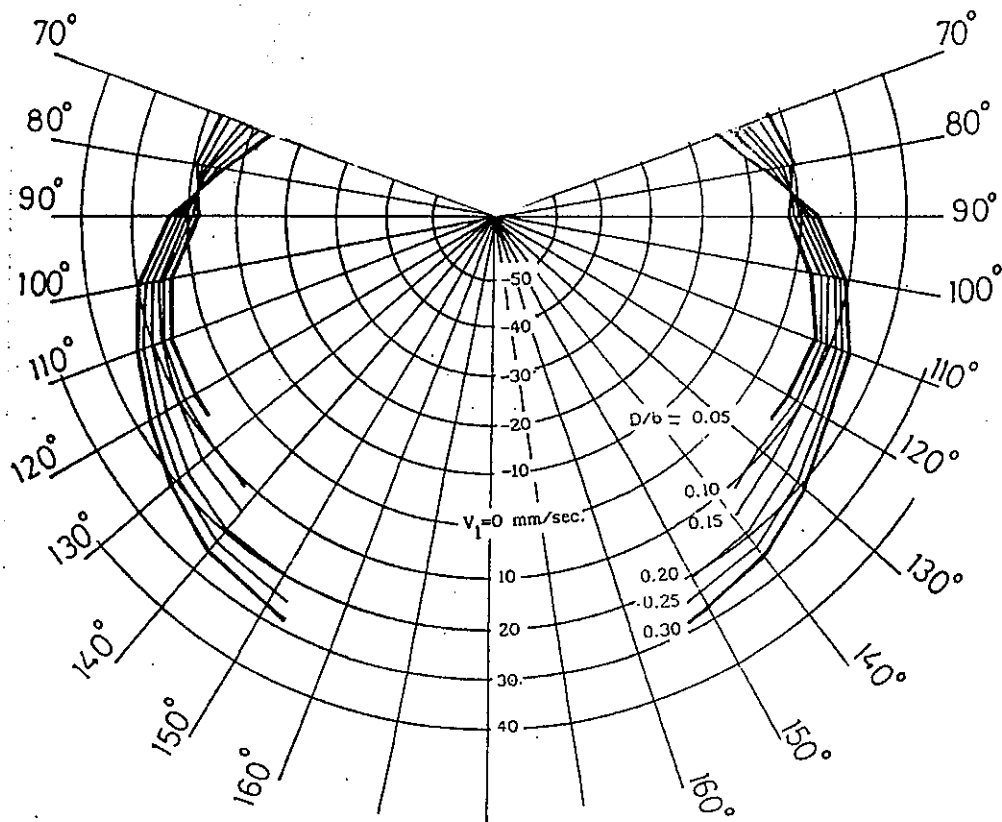


Fig. 5: local velocity distribution around the cylinder  
 for different diameter ratios at mean velocity  
 of  $V_m = 2$  mm/sec.

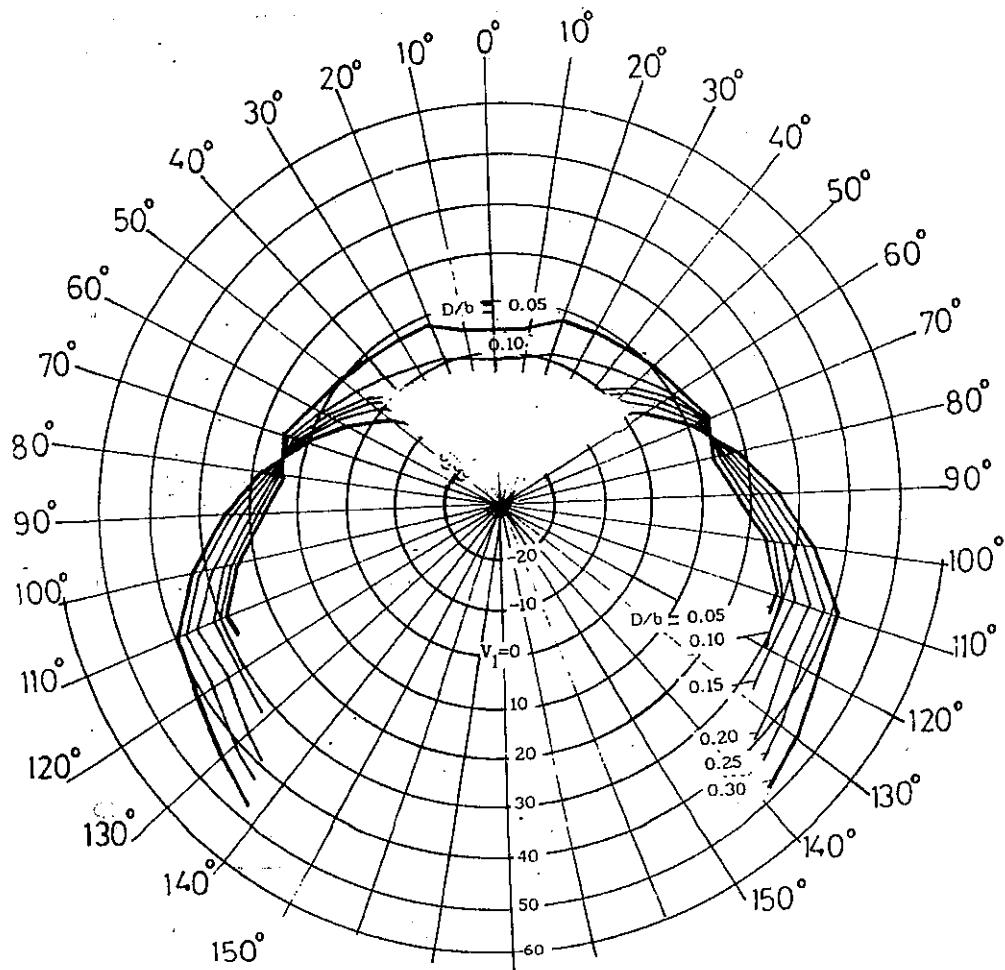


Fig. 6: local velocity distribution around the cylinder for different diameter ratios at mean velocity of  $V_m = 18$  mm/sec.

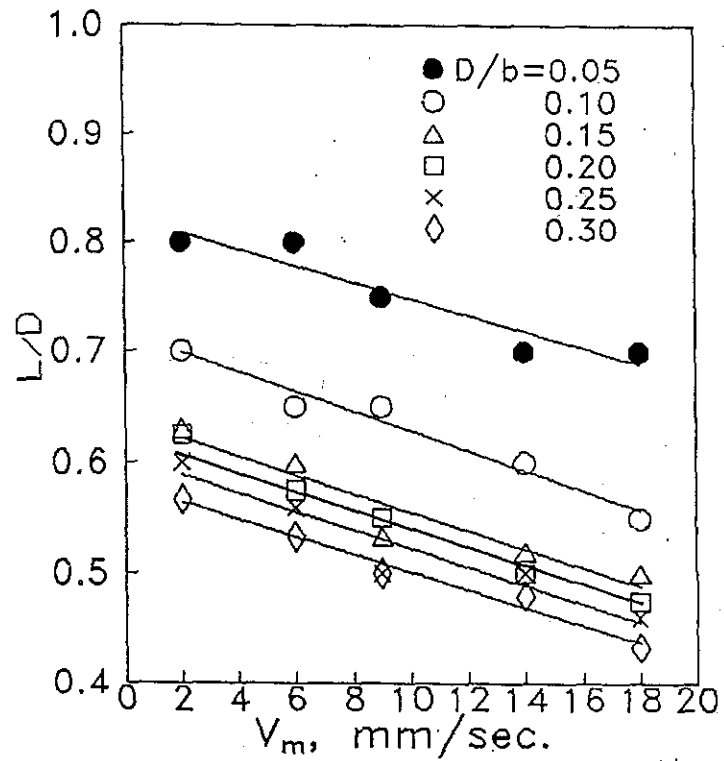


Fig.7: Effect of diameter ratio  $D/b$  on the height to cylinder diameter ratio  $L/D$  for the dead region.

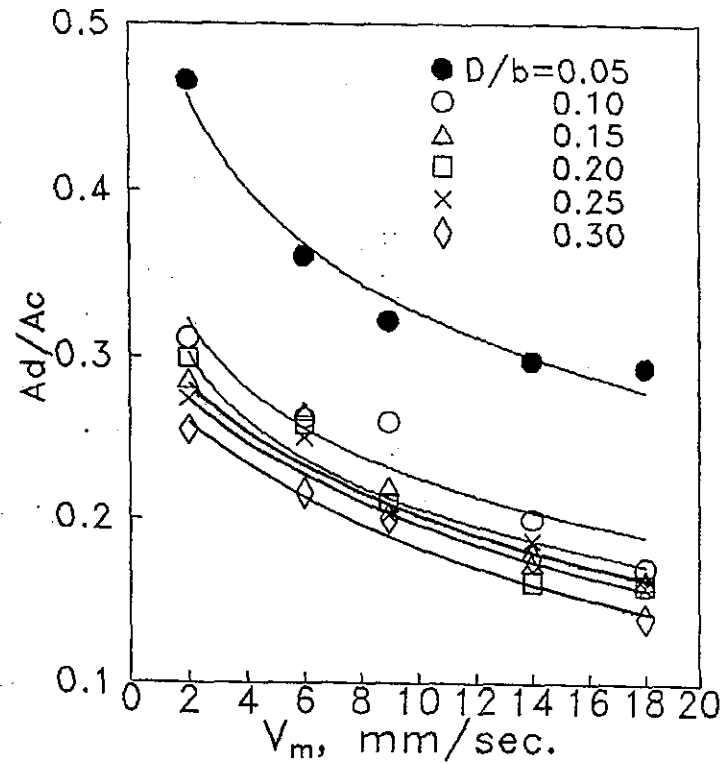


Fig.8: Effect of diameter ratio  $D/b$  on the dead to cylinder diameter areas ratio  $A_d/A_c$  for the dead region.



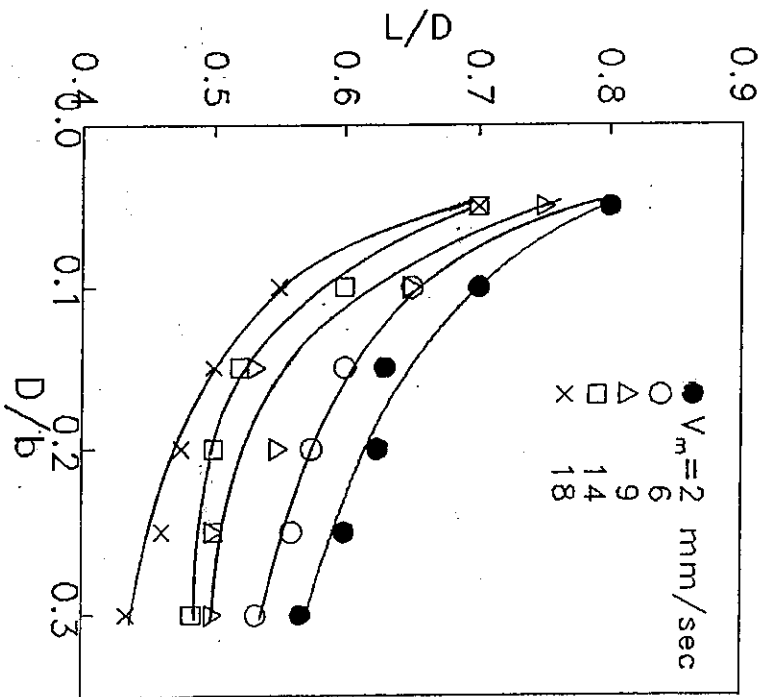


Fig.9: Effect of layers mean velocity  $V_m$  on the height to cylinder diameter ratio  $L/D$  for the dead region.

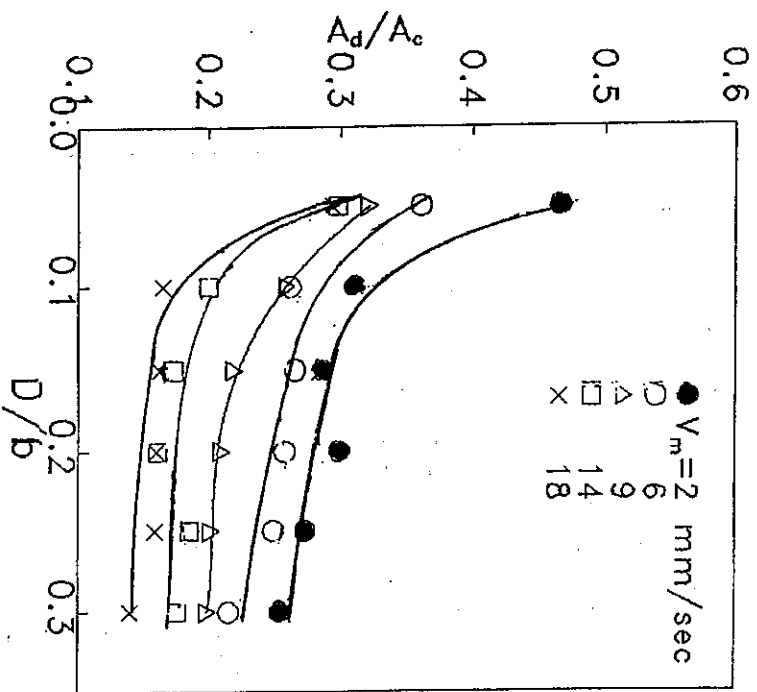


Fig.10: Effect of layers mean velocity  $V_m$  on the dead to cylinder diameter areas ratio  $A_d/A_c$  for the dead region.

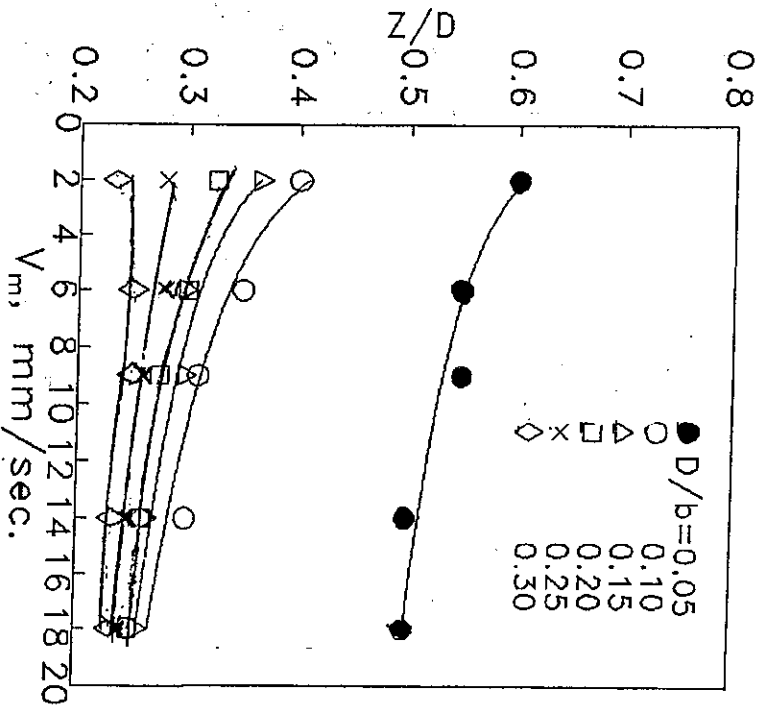


Fig.11: Effect of diameter ratio  $D/b$  on the depth to cylinder diameter ratio  $Z/D$  for the rear air region.

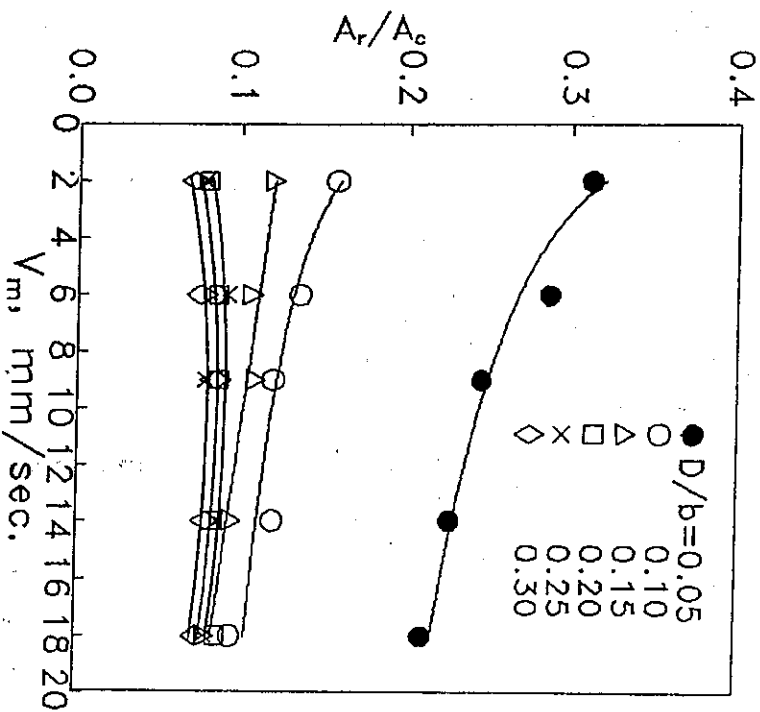


Fig.12: Effect of diameter ratio  $D/b$  on the rear to cylinder areas ratio  $A_r/A_c$  for the rear air region.

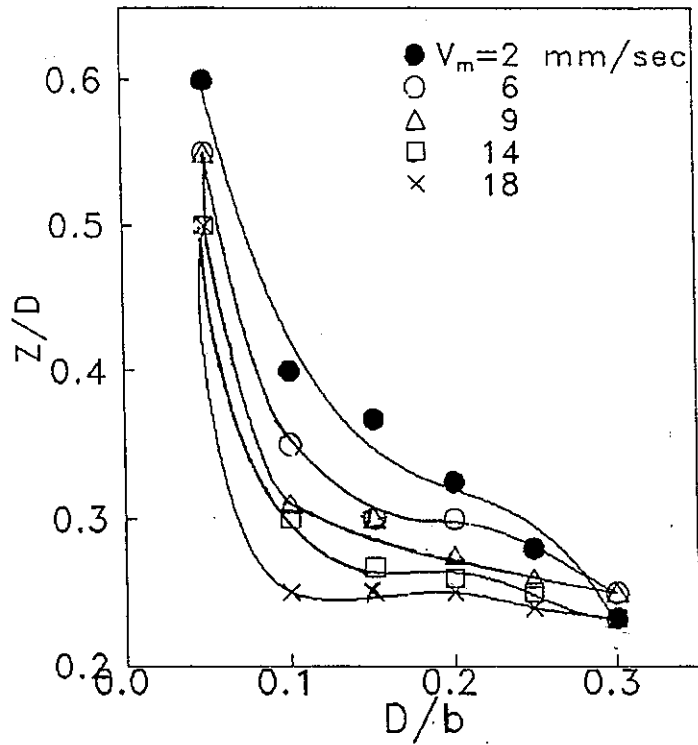


Fig.13: Effect of layers mean velocity  $V_m$  on the depth to cylinder diameter ratio  $Z/D$  for the rear air region.

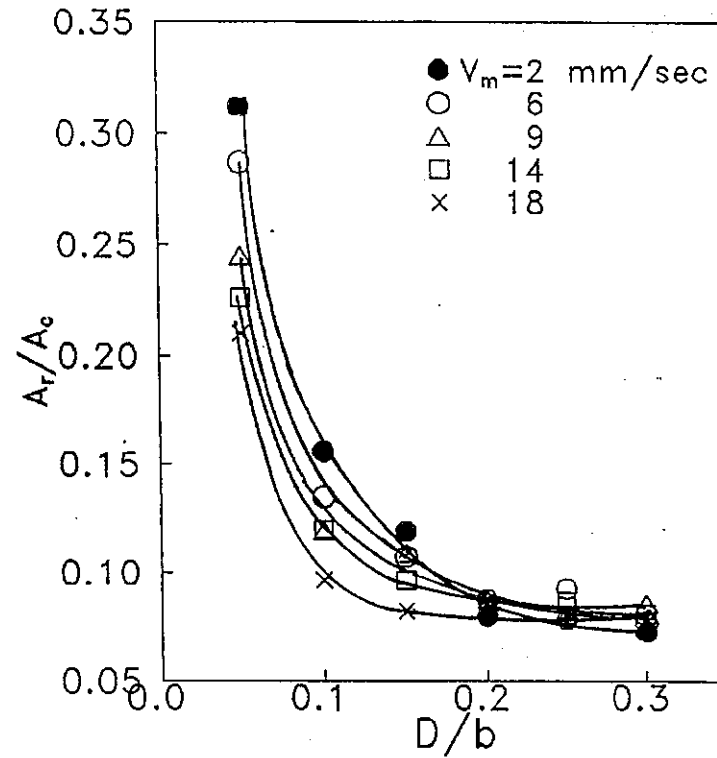


Fig.14: Effect of layers mean velocity  $V_m$  on the rear to cylinder areas ratio  $A_r/A_c$  for the rear air region.

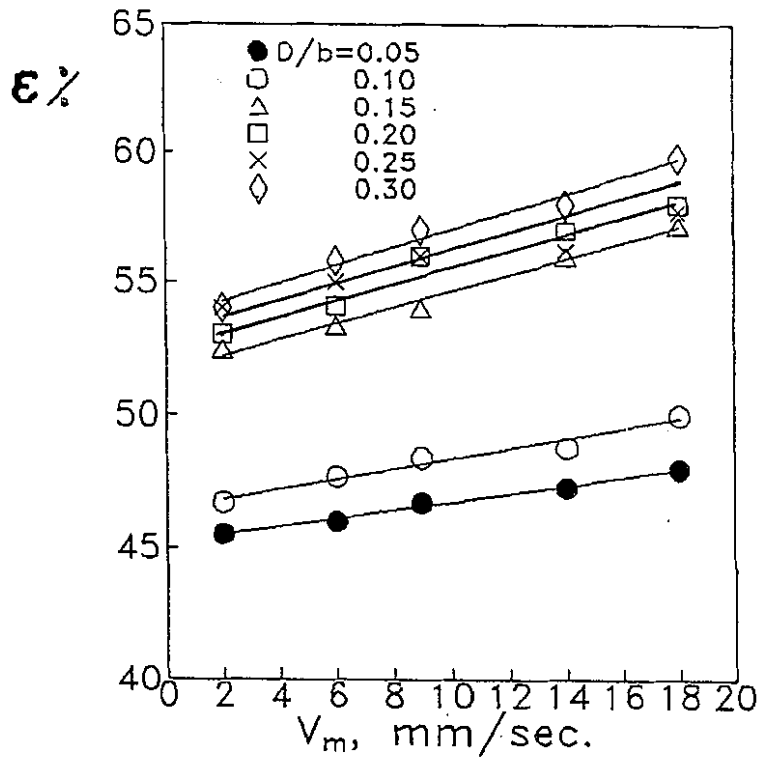


Fig.15: Effect of diameter ratio  $D/b$  on the effective working surface  $\varepsilon$

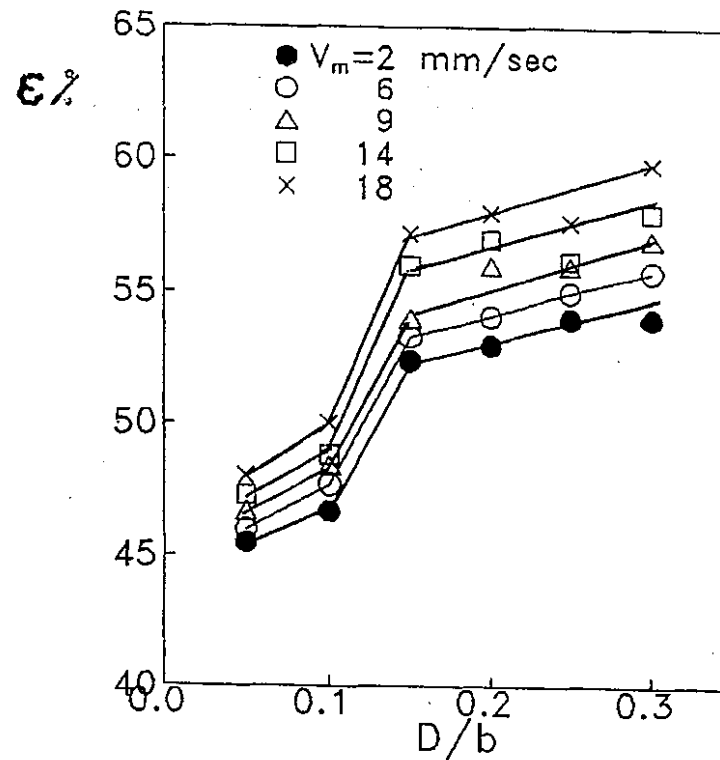


Fig.16: Effect of layers mean velocity  $V_m$  on the effective working surface  $\varepsilon$

بحوث تجريبية  
لدراسة خصائص سريان الأجام الصلبه حول الأسطح الاسطوانية

مقدم من

د/ محمد عبد الوارث حبيب      د/ شديد حسن شمس الدين

كلية الهندسة - جامعة المنوفية

المخلصى :-

تمت دراسته تجريبية لسريان الأجام الصلبه حول الأسطح الاسطوانية واستخدم الأرز كمونج للماده الصلبه - تم بحث أثر كل من سرعة الحبوب - وقطر السطح الأسطوانى على الأبعاد الهندسية للمنطقة الساكنه ومنطقة الهوائ الخلفية والسطح العامل الفعال .

تم أيضا مناقشة مجال السريان عن طريق الدراسة المرئية وتم الحصول على توزيع السرعات حول أسطح الأسطوانات مختلفة الأقطار من نمونج السريان المنتج بواسطه طريقه الأثر الأسود .

تغيرت سرعة الحبوب المتوسطه من ٢ الى ١٨ م/ث واستخدمت الأسطح الاسطوانيه بأقطار من ١٠ - ٦٠ مم .

أظهرت النتائج أن خصائص السريان تعتمد بدرجة كبيرة على كل من سرعة الحبوب المتوسطه وقطر الاسطوانيه .